

Electronic Energy Transfer within the Hexamer Cofactor System of Bacterial Reaction Centers

Marten H. Vos,^{*,†} Jacques Breton,[‡] and Jean-Louis Martin[†]

Laboratoire d'Optique Appliquée, INSERM U451, Ecole Polytechnique-ENSTA, 91761 Palaiseau Cedex, France, and SBE/DBCM, CEA de Saclay, 91191 Gif-sur-Yvette Cedex, France

Received: April 30, 1997; In Final Form: September 9, 1997[©]

Flow of excitation energy within the bacteriochlorin cofactor system of bacterial reaction centers has been studied by multicolor transient absorption spectroscopy using differently shaped excitation pulses of 30 fs, both at room temperature and at 15 K. This approach, which includes the analysis of free induction decay signals, helps to disentangle the processes of electronic dephasing, energy transfer, internal conversion, and nuclear motion, all taking place on the time scale of ~ 100 fs. Part of the excitations (estimated at 80–90% at room temperature) flow via the scheme $H^* \rightarrow B^* \rightarrow P_+^* \rightarrow P_-^*$, in which H^* and B^* represent excited bacteriopheophytin and bacteriochlorophyll monomers and P_+^* and P_-^* the upper and lower excited states of the bacteriochlorophyll dimer P, respectively. $H^* \rightarrow B^*$ takes less than 100 fs. $B^* \rightarrow P_+^*$ (~ 200 fs) energy transfer is a slower process than the internal conversion process within P^* (50–100 fs) and therefore is rate limiting for P_-^* formation. At low temperature, electronic dephasing associated with the B^* and P_+^* states takes place on a similar time scale as P^* internal conversion. Upon excitation with pulses centered at 820 nm, estimated to spectrally overlap the close-lying B and P_+ bands to equal extent, more than 90% of the P_- band bleaches instantaneously and $B^* \rightarrow P^*$ transfer occurs for less than 10%. This might be indicative of an unexpectedly strong contribution of P_+ to the 800 nm band. Alternatively, we propose that under these conditions the strongly coupled B^* and P_+^* states are coherently excited. This possibility is consistent with $B^* \rightarrow P_+^*$ electronic energy transfer occurring in the strong coupling regime under conditions where B^* is more selectively populated. The observed time scales are temperature-insensitive and furthermore similar in *Rhodobacter sphaeroides* R26 and *Rhodospseudomonas viridis*, which eliminates the possibility of direct $B^* \rightarrow P_-^*$ energy transfer. At room temperature, part of the excitation energy flow deviates from the above scheme (Lin, S.; Taguchi, A. K. W.; Woodbury, N. W. *J. Phys. Chem.* **1996**, *100*, 17067–17078), resulting in excitation-wavelength-dependent distributions of excited and/or radical pair states on the picosecond time scale. In general agreement with previous low-temperature work on a mutant reaction center (van Brederode, M. E.; Jones, M. R.; van Mourik, F.; van Stokkum I. H. M.; van Grondelle, R. *Biochemistry* **1997**, *36*, 6855–6861), we found that this deviation is particularly strong (up to $\sim 50\%$) at low temperature. Upon excitation in H and B, a high quantum yield is observed of radical pairs involving H_L , with characteristics in the $H_L Q_Y$ region, differing from those of $P^+H_L^-$ and suggesting that they can be identified as $B_L^+H_L^-$.

1. Introduction

The reaction center (RC) of purple bacteria is a membrane-bound pigment–protein complex that is generally considered as a model system for biological electron transfer. Its pigment system is arranged in a near- C_2 symmetry and contains six bacteriochlorin cofactors with Q_Y transitions in the near-infrared. In the case of *Rhodobacter sphaeroides* and several related species, these cofactors give rise to three well-separated Q_Y absorption bands, termed P, B, and H. The number of transitions contributing to each band in the absolute absorption spectrum is very limited (at most three; see below). Furthermore, only one transition underlies the lowest-lying P band, the lower-exciton transition P_- of the primary donor bacteriochlorophyll (Bchl) dimer P. These features contrast with the RC of photosystem II where the absorption of the six to eight cofactors is highly congested and with the RC of photosystem I and of green sulfur bacteria, which contain many more pigments. Thus, apart from studying electron transfer, the RC of purple bacteria also offers unique possibilities of spectro-

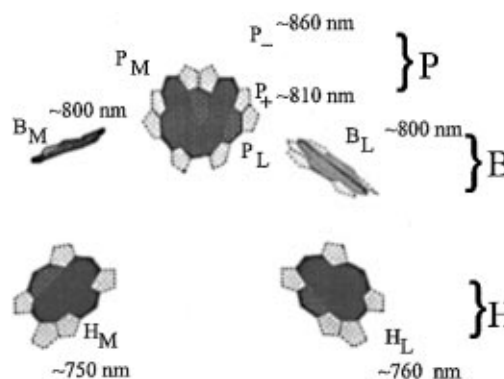


Figure 1. Arrangement and nomenclature of the bacteriochlorophyll (P_L , P_M , B_L , B_M) and bacteriopheophytin (H_L , H_M) cofactors and the corresponding transitions (P_- , P_+ , B_L , B_M , H_L , H_M) to the excited states (denoted with * throughout the paper). Indexes are not used where no distinction between L and M chains or upper and lower excited states can be made. The approximate positions of the transitions at room temperature are indicated.

* To whom correspondence should be addressed. FAX: 33 160106085. E-mail: vos@ensta.fr.

[†] Ecole Polytechnique-ENSTA.

[‡] CEA de Saclay.

[©] Abstract published in *Advance ACS Abstracts*, November 1, 1997.

scopically resolving downhill energy transfer in a well-defined chromophore system by selective excitation.

Figure 1 shows the arrangement of the pigments along with a glossary of the nomenclature of the Q_Y transitions and states

used in this paper. The B band (~ 800 nm) mainly contains the transitions from the two "accessory" Bchls B_L and B_M as well as a contribution, generally considered relatively weak, from the higher exciton component P_+ of P, on the red side of this band. The H band (~ 760 nm) contains the transitions from the two bacteriopheophytins (Bpheo) H_L and H_M . H_L , which absorbs somewhat more to the red than H_M , is thought to be the primary electron acceptor.¹ B_L may act as a real or virtual electron carrier intermediate in the $P^* \rightarrow P^+H_L^-$ reaction^{2,3} (* denotes excited states), which takes ~ 3 ps at room temperature (RT)^{4,5} and ~ 1 ps at cryogenic temperatures.⁶

Pump-probe experiments performed over a decade ago with pulses of ~ 150 fs⁷⁻⁹ could not time-resolve the energy transfer from excited H (H^*) and B (B^*) to excited P (P^*), indicating that it takes less than 100 fs. This is more than an order of magnitude faster than the rates expected¹⁰ on the basis of weak-coupling Förster¹¹ theory, perhaps not surprisingly suggesting that the weak coupling approximation is not appropriate for describing this system. In the early B-band excitation experiments, a 400 fs kinetic phase in the B-band region not related to energy transfer to P^* was also observed.^{7-9,12} It has been demonstrated very recently¹³ that this phase was due to the artifactual buildup of a steady-state population of the oxidized primary donor.

Apart from the measurement of a ~ 200 fs rise time in P_-^* emission upon excitation in the Bchl Q_X band,¹⁴ experiments in which energy transfer or internal conversion were resolved have been performed in very recent years. Stanley et al.¹⁵ monitored low-temperature P_-^* spontaneous fluorescence at 940 nm upon excitation in the B and H bands and observed rise times of ~ 80 , ~ 150 , and ~ 250 fs when exciting at 825 nm (P_+), 804 nm (B), and 759 nm (H), respectively, in agreement with an early report by Fleming's group.¹⁶ Jonas et al.¹³ performed one-color pump-probe experiments in the B band, which were interpreted in terms of two-step energy transfer following the scheme



Haran et al.¹⁷ excited at 810 nm and probed at three individual wavelengths in the near- and mid-infrared. The ~ 100 fs phase observed in these experiments was ascribed to $B^* \rightarrow P_-^*$ energy transfer. These studies all agree with the fact that the overall energy transfer from B^* to P_-^* takes roughly 150 fs. However, there is no consensus on the mechanism that governs this process. A B^*/P_-^* weak-coupling Förster mechanism,¹⁷ or alternatively a B^*/P_+^* strong-coupling Förster mechanism^{13,15} followed by P^* internal conversion,¹⁵ has been proposed. A third mechanism involved internal conversion from a mixed B^*/P_+^* state.¹⁷ Mechanisms involving strong coupling between B and P_+ are invoked by all these authors. Such mechanisms would lead to intrinsically nonexponential kinetics.¹⁵ Additional complications arise from the fact that on the time scale of energy transfer the excited states are certainly not vibrationally relaxed¹⁸⁻²⁰ and that electronic dephasing may take place on the same time scale.²¹

In the above experiments, kinetic schemes are derived from measurements using probes at single wavelengths. In principle, much more information can be obtained when the probe is spectrally resolved, especially by comparing different excitation conditions. Such an approach was taken by Lin et al.,²² employing spectrally narrow, relatively long (150 fs) excitation pulses. They showed that, whereas substantial energy transfer indeed takes place in the 100–300 fs time range, the transient spectra are moderately excitation-wavelength-dependent, even

on the picosecond time scale. They challenged the validity of an analysis in terms of simple rate schemes and proposed a near-adiabatic mechanism of energy and electron transfer, with possible different pathways for formation of the primary photoproduct. More recently, for the YM210W mutant at low temperature, van Brederode et al. proposed a mechanism of charge separation without P^* formation on the basis of fluorescence excitation spectra²³ and strongly excitation wavelength-dependent absorption spectra on the picosecond time scale.²⁴

The present work aims at a more detailed assessment of the energy transfer and internal conversion processes in relation to the primary charge separation and vibrational coherence. We combine multicolor spectroscopy with a high (30 fs) time resolution, which allows us to both time- and spectrally resolve processes taking place in the femtosecond and picosecond time scale. Performing the experiments both at room temperature and at cryogenic temperature, where the bands are better separated, further helps to assign the spectroscopic observables. To understand the role of the upper exciton component of P_+ , we compared excitation selectively into the P_+ band, at 820 nm, with excitation directly in P_- at 880 nm and with excitation in the H and B bands, at 770 nm. The perturbed free induction decay signal observed under specific experimental conditions is characterized separately. This signal is of importance because it gives independent information on the electronic dephasing time. Results on RCs from both *R. sphaeroides* R26 and *Rhodospseudomonas viridis* are presented.

2. Materials and Methods

Isolated RCs of *R. sphaeroides* strain R26⁴ and *Rps. viridis*²⁵ were prepared as described. For *R. sphaeroides* R26, 50 mM dithiothreitol was added to prereduce the quinone electron acceptor Q_A . For *Rps. viridis*, Q_B binding was inhibited by the addition of 100 μ M stigmatellin and the cytochrome hemes were oxidized by a mixture of potassium ferricyanide and potassium ferrocyanide (10 mM each), leaving P essentially reduced.²⁶ The RCs were suspended in 20 mM Tris buffer, pH 8.0. For measurements at 15 K, they were mixed with 67% glycerol (v/v). The concentration of the samples was adjusted to an optical density of ~ 0.4 at the excitation wavelength (optical path length 1 mm). The 15 K measurements were performed in a convection cryostat.

The general arrangement of the femtosecond spectrometer, operated at 30 Hz, was as described previously.^{19,27} Pump pulses with a fwhm of ~ 30 fs, centered at 940, 880, 820, or 770 nm were generated using the dyes LDS 925, LDS 867, LDS 821, and LDS 765, respectively, as an amplification medium for the continuum. The continuum probe beam was compressed to a chirp of less than 15 fs over a wavelength range of ~ 60 nm near 800 nm or ~ 80 nm near 920 nm, as monitored by the induced birefringence observed when the sample cell was replaced by a CS_2 cell. The pump and probe beams were polarized at the magic angle (54.7°) in order to avoid photo-selection effects. The intensity of the pump beam was adjusted so that less than 20% of the RCs was excited upon each shot.

3. Results and Interpretation

3.1. Perturbed Free Induction Decay. Pump-probe absorption spectroscopy under conditions where the electronic dephasing time of the probed transitions is of the same order as the temporal resolution gives rise to a signal at negative delay times. This signal is due to the perturbation, by the pump pulse, of the decay of the polarization induced in the medium by the

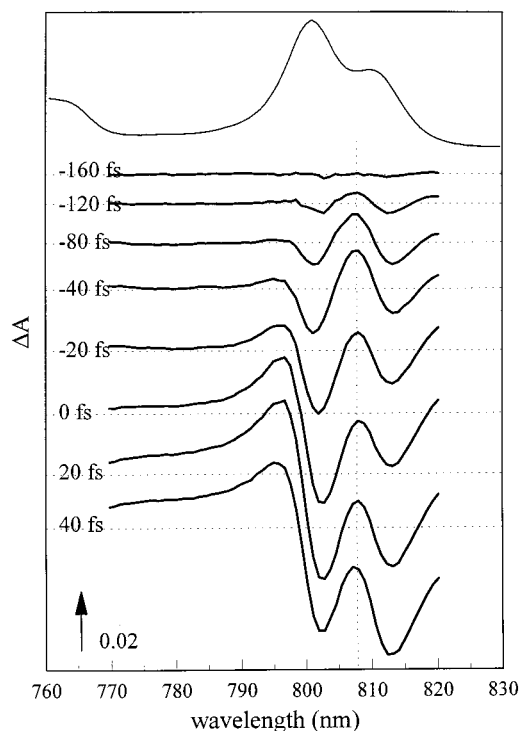


Figure 2. Perturbed free induction decay. Transient spectra of *R. sphaeroides* R26 RCs at 15 K, upon excitation at 820 nm, at negative (probe pulse precedes pump pulse) and near-zero positive delay times. The chirp in this spectral region is less than 10 fs. Upper panel shows the ground-state absorption spectrum.

probe pulse ("perturbed free induction decay").^{28–30} Under the experimental conditions of the present work, such signals are resolved.

As an example, Figure 2 shows the transient absorption spectra in the B-band region at negative and near-zero delay times for *R. sphaeroides* R-26 RCs at 15 K under excitation with 30 fs pulses centered at 820 nm. Even at delay times where the probe pulse precedes the pump pulse by more than 100 fs, i.e., clearly outside the temporal region where the pump pulse and the probe pulse overlap, a transient spectrum is observed. It is characterized by spectral oscillations, which decrease in amplitude and increase in frequency with increasingly negative pump–probe delay time, as expected for a perturbed free induction decay signal.^{28,29} Near $t = 0$, the signal is superimposed on the population response of the sample.

For a two-level system, it is expected that the perturbed free induction decay signal gives rise to a bleaching at the maximum of the absorption band, which decays exponentially with the probe–pump delay.²⁸ The 800 nm ground-state band of *R. sphaeroides* R-26 RCs at 15 K (Figure 2) is composed of two bands with maxima at 801 and at ~811 nm, respectively. As expected, the negative delay signal clearly shows a bleaching near the centers of both bands. We fitted the kinetics (not shown) at the center wavelengths of these bleachings (802 and 812 nm) with a function of the form

$$[\Theta(-t)A_{-1}e^{t/\tau_{-1}} + \Theta(t)(A_1e^{-t/\tau_1} + A_2e^{-t/\tau_2} + A_3)] \otimes I(t) \quad (1)$$

in which $\Theta(t)$ is the Heaviside function and $I(t)$ is the instrument response function, which is the convolution of the pump and the probe signals. We found a value for τ_{-1} of ~50 fs at 802 nm and ~80 fs at 812 nm. Gaussian deconvolution of the absorption band gave spectral widths of ~130 cm^{-1} (8 nm) of the individual bands, which correspond, assuming a homoge-

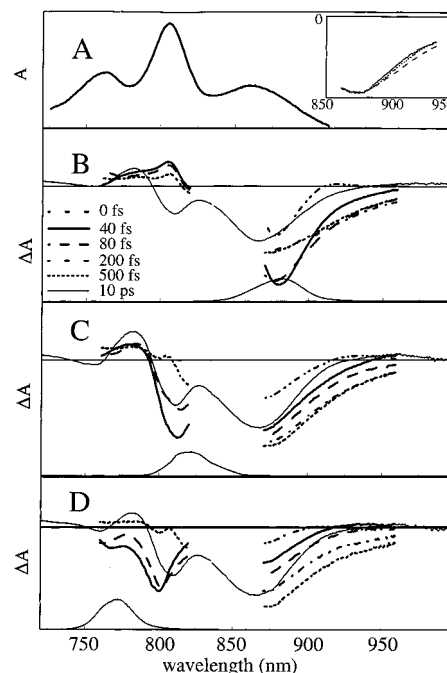


Figure 3. Ground-state (A) and transient (B–D) spectra at selected delay times of *R. sphaeroides* R26 RCs at room temperature. Maxima of the excitation pulses were at 880 nm (B), 820 nm (C), and 770 nm (D). The spectral profiles of the pump pulses are drawn at the bottom of each panel. The spectra in each panel were taken in two parts: one where the probe was compressed at ~800 nm and one where the probe was compressed at ~920 nm. The spectra of the two parts are normalized to the overlapping 800–860 nm spectral range at 10 ps. For the subpicosecond delay times, only the spectral region where the chirp was less than 15 fs is shown. For clarity, in the blue region only the 40, 80, and 500 fs and the 10 ps spectra are shown. The inset in panel A shows transient spectra after 0.7 ps in the 860–930 nm spectral range upon excitation at 880 nm (---), 820 nm (···), and 770 nm (—). These spectra are normalized at 860 nm.

neously broadened band, to T_2 times of ~80 fs, in good agreement with the perturbed free induction decay signals.

At wavelengths outside the maxima of the ground-state bands, the kinetics are expected to decay in an oscillatory manner as a function of negative delay time. As expected, the initial decay was faster at these wavelengths, but with the time resolution of ~30 fs the oscillations at $t < 0$ were strongly damped, and the kinetics could be reasonably described with an exponential function.³¹

At RT, the signal in the B band at negative delay times was much smaller than at 15 K, which would be consistent with a faster dephasing time (indeed, a T_2 of ~20 fs was reported from two-pulse photon echo experiments³²). A weak signal at negative delay times also complicated the kinetics in the 760 nm region where the bacteriopheophytins absorb, and was also present at RT.

It is known that the shape and intensity of the perturbed free induction signal depend on the detuning of the pump from the resonance.²⁹ In the P₋ band region a (small) signal at negative delay times was resolved only if excitation occurred directly in this band. As reported before,¹⁹ in this band a strong signal during the pump–probe temporal overlap is observed, possibly due to (at least in part) an optical Stark effect.

3.2. *R. sphaeroides* R-26 at Room Temperature. Figure 3 shows an overview of the RT transient spectra of *R. sphaeroides* R-26 RCs obtained in the 700–1000 nm spectral range. At each excitation wavelength (880, 820, and 770 nm), the spectra were obtained from experiments using two different probe-shaping conditions. These were respectively optimized

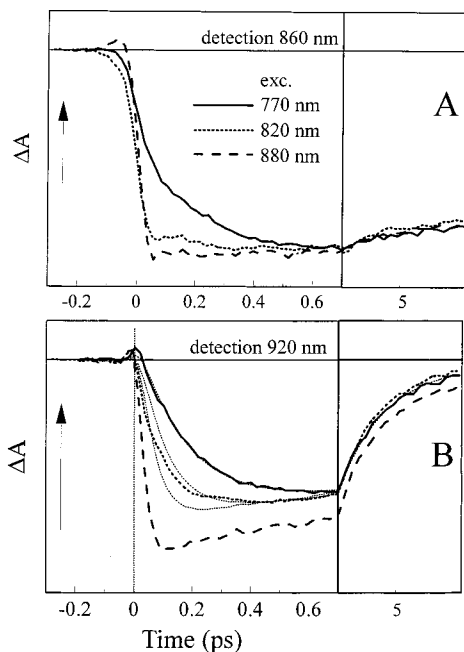


Figure 4. Kinetics of *R. sphaeroides* R26 RCs at room temperature at 860 nm (A), where bleaching of P is mainly monitored, and at 920 nm (B), where P* stimulated emission is mainly monitored. Excitation is at 880 nm (---), 820 nm (···), and 770 nm (—). The kinetics are normalized to that at 860 nm, 0.7 ps. In panel B are also shown (···) a fit of the 770 nm data with a rise time of 180 fs and a decay time of 3.5 ps and the 880 nm excitation kinetics convoluted with rise times of 50 and 100 fs, normalized to the 820 nm data. The vertical arrows in each panel represent identical absorption changes. Note the different time scales.

for 870–950 nm, the spectral region covering the lower exciton band of P and P* stimulated emission (SE), and for 760–820 nm, the spectral region covering the “monomeric” bacteriochlorins. For both sets of experiments, the total spectral range recorded was ~250 nm wide and extends to regions where the pulse is significantly chirped. In Figure 3, only the data in the essentially chirp-free spectral regions are shown for the subpicosecond delay times.

In both regions, the spectral evolution is strongly excitation wavelength-dependent on the time scale of a few hundred femtoseconds. It is clear that excitation (at 770 and 820 nm) in the H, B, and P₊ bands leads, within a few hundred femtoseconds, to the depletion of the ground state of P, as witnessed by the bleaching of the P₋ band centered at 870 nm, and to the formation of P*, as witnessed by the appearance of the SE signal centered at ~920 nm. This is in general agreement with other recent reports.^{13,15,17,22} The spectral and temporal resolution of the present study allows a more detailed assessment of the pathways of energy transfer and internal conversion leading to P* from the initially photoformed excited states. By contrast to single wavelength measurements where it is usual to perform analyses with exponential functions,^{13,15–17} this has appeared impossible for multicolor experiments.²² In our case, attempts to globally fit the data sets in terms of decay-associated spectra using a procedure described previously³³ also did not yield satisfactory results. This was in part due to intrinsic nonexponentialities related to (a) the expected coherences in the kinetics at positive delay times (clearly for the 880 nm excitation data and to a lesser extent for the other excitation conditions) in both the 800³⁴ and the 920 nm regions³⁵ and (b) the wavelength-dependent perturbed free induction decay (see section 3.1). Furthermore, some of the fits tended to converge to unstable solutions with close-lying time constants and opposite amplitudes. This indicates that if at all the underlying

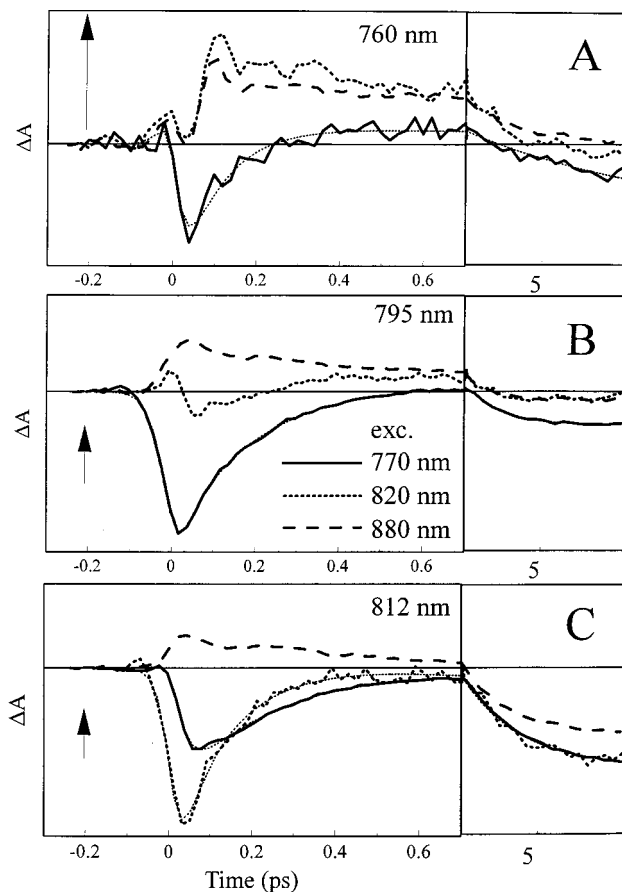


Figure 5. Kinetics of *R. sphaeroides* R26 RCs at room temperature at 760 nm (A), 795 nm (B), and 812 nm (C). Excitation is at 880 nm (---), 820 nm (···), and 770 nm (—). The kinetics are normalized as in Figure 3. Superimposed on some kinetics are exponential fits (···). The subpicosecond time constants for the 770 nm excitation data are the following: (760 nm) 100 fs; (795 nm) 30 fs (30%) and 220 fs (70%); (812 nm) 30 fs (rise of bleaching) and 270 fs (decay of bleaching). The decay of the 820 nm excitation, 812 nm probe kinetics is fit with a 120 fs time constant. The vertical arrows in each panel represent identical absorption changes. Note the different time scales.

processes are exponential processes, their rate constants are near-degenerate. To avoid these problems, our kinetic analysis is based on a comparison of kinetics at key wavelengths obtained under different excitation conditions. As a guide, we have superimposed fitted exponential kinetics in some cases.

Figure 4 shows kinetics at 860 nm, i.e., near the maximum of the P₋ absorption band, and at 920 nm, near the maximum of the P* emission band associated with the lower excited state (P₋*) of the dimer P. Figure 5 shows kinetics near the maximum of the H absorption band (760 nm) and at the blue (795 nm) and red (812 nm) side of the B absorption band. At the latter wavelength a contribution from the upper exciton transition of the dimer P (P₊) is also expected.³⁶ In the following we will describe the relevant features in the spectral evolution upon the different excitation conditions displayed in Figures 3–5.

3.2.1. No 400 fs Phase. In previous work,^{7–9,12} a strong 400 fs (1/e time) decay phase of the bleaching in the B-band region has been observed upon excitation into transitions at energies higher than those of P. This phase was due to artifactual energy transfer to P⁺.¹³ Under our present conditions, where Q_A is prereduced, charge recombination should be completed between two laser shots (33 ms), and the appearance of this phase through the buildup of a population of P⁺ should be avoided. Upon excitation at 820 nm, a bleaching centered at 812 nm appears, the decay of which is completed at $t = 400$

fs (part C of Figure 3 and parts B and C of Figure 5). The kinetics at 812 nm can be reasonably described with time constants of 120 fs (decay of the initial bleaching) and 3 ps (induced bleaching, presumably due to $P^+H_L^-$ formation) (Figure 5C), and in particular, no other exponential components were needed for a reasonable fit in the 400 fs to 10 ps time range. We also note that the 120 fs time constant perfectly corresponds to the reported magic angle decay time for RT one-color pump–probe experiments in the B band, obtained under conditions where the RCs were completely relaxed prior to the excitation pulse.¹³ Upon excitation at 770 nm, the decay of the bleaching in the B-band region also proceeds significantly faster than 400 fs (parts B and C of Figure 5) (but slower than upon excitation at 820 nm because of slower overall energy transfer; see below). Altogether, we conclude that under our conditions artifactual buildup of P^+ does not contribute to our data.

3.2.2. Downhill Energy Transfer from H^* . From a Gaussian deconvolution of the ground-state absorption spectrum we estimate that the 770 nm pump pulse initially creates H^* and B^* in a ratio of $\sim 3:1$ (not shown). Accordingly, excitation at 770 nm generates an initial bleaching of both the H band and the B band (Figure 3D). The decay of the initial bleaching in the H spectral region (<780 nm) presumably reflects decay of initially populated H^* . This decay is completed within ~ 300 fs. Figure 5A shows a fit of the kinetics at 760 nm with a time constant of 100 fs. It is more difficult to establish the H^* population decay on faster time scales because of contributions of electronic coherence signals in the H-band region during the pump–probe temporal overlap. However, we note that, whereas the 770 nm pulse preferentially excites H, at 40–80 fs (immediately after the pump pulse) the bleaching in the B-band region is much stronger than the bleaching in the H-band region. This indicates that a significant part of H^* decays on a time scale comparable with or faster than the pulse length (30 fs). In summary, following direct excitation of the H pigments with 770 nm pulses, H^* decays in ~ 100 fs or faster.

The population of P^* is monitored by the appearance of a bleaching of the P_- ground-state band centered at 860 nm and of P_-^* SE centered at ~ 920 nm. Upon excitation at 770 nm, the maximum bleaching in this region occurs only after ~ 700 fs, significantly later than the completion of H^* decay. At 920 nm, corresponding to the maximum of the SE band where the effect of oscillatory features due to P_-^* vibrational motions is minimized,^{35,37} the rise kinetics are reasonably well described with an exponential function with a time constant of 180 fs (inset of Figure 3A, Figure 4B). This indicates that energy transfer to P_-^* occurs in this time range. From the difference in time scales of H^* decay (100 fs or less) and P_-^* rise (~ 200 fs), we conclude that energy transfer does not occur directly from H^* to P_-^* . Therefore, intermediate excited states, presumably B^* or the upper exciton excited state of P (P_+^*), must be transiently populated. B^* is expected to give rise to a negative signal at ~ 800 nm due to bleaching of the B band and SE. P_+^* is expected to give rise to bleaching of the P_+ band at ~ 810 nm and its associated SE and to bleaching of the P_- band at 860 nm, such as that observed at early times upon excitation with a 820 nm pulse (Figure 3C). Upon excitation at 770 nm, on the 40–80 fs time scale the main bleaching is centered at ~ 800 nm (Figure 3D). At these times, this bleaching is much stronger than both the H-band and P_- -band bleaching. Assuming that the B and H bands are not strongly coupled,⁴⁰ this strongly suggests that B^* is the most highly populated electronic state. Taking into account that the 770 nm pulse is estimated to populate 75% H^* and 25% B^* (see above), this

indicates that B^* is populated from H^* .⁴¹ This conclusion is in agreement with results using more selective excitation in the H band with spectrally narrower, 150 fs pulses.²² However, it cannot be excluded that some H^* decays directly to P_+^* .

3.2.3. Downhill Energy Transfer from B^* . Upon excitation at 770 nm, the overall decay of B^* , as monitored by the decay of the bleaching at ~ 800 nm, occurs roughly on a time scale of ~ 200 fs (part D of Figure 3 and parts B and C of Figure 5). This time corresponds well with the appearance of the ground-state bleaching of P_- and P_-^* SE (Figure 4), and we conclude that $B^* \rightarrow P_-^*$ transfer takes in ~ 200 fs.

In principle, $B^* \rightarrow P_-^*$ transfer may proceed either directly or via P_+^* . Upon excitation at 770 nm, the P_- band at 860 nm (expected to bleach if either P_-^* or P_+^* is populated) bleaches somewhat faster than the appearance of SE at 920 nm (associated with P_-^* only). Furthermore, on the time scale of tens of femtoseconds, the position of the bleach in the B-band region shifts to the red and in particular develops a wing at the red side of the B band, where P_+ is thought to absorb. These two observations are consistent with a model in which energy transfer toward P_+^* precedes $P_+^* \rightarrow P_-^*$ internal conversion. A more quantitative analysis of these observations is complicated by the intrinsic modulation by low-frequency nuclear dynamics of the P_-^* SE^{22,42} and in principle also of the B^* SE, although low-frequency modes are much less coupled to B^* formation.^{43–45}

The roughly concomitant decay of B^* and appearance of P_-^* indicate that if P_+^* is formed from B^* , it must decay faster than it is formed (see section 3.2.4). Consequently, a high transient population of P_+^* cannot be expected. Indeed, under excitation at 770 nm, at no time is a transient spectrum similar to that observed at early times under selective excitation of P_+ at 820 nm observed (Figure 3).

3.2.4. P^* Internal Conversion. The 820 nm pulse selectively excites the P_+ transition, as well as the B transitions and the high-energy tail of the P_- transition. Upon excitation at 820 nm, a bleaching centered at 812 nm appears, indicating that indeed P_+ (maximum ~ 810 nm) is excited to a significant extent. Concomitantly, $\sim 90\%$ of the final P_- -band bleaching appears instantaneously (deconvoluted rise time of <20 fs at 860 nm); the remainder appears within a few hundred femtoseconds (Figure 4A). Since $B^* \rightarrow P^*$ energy transfer is slower than 20 fs, this would imply that the 820 nm excitation pulse excites P directly in $\sim 90\%$ of the RCs (see Discussion).

The initial bleaching of the P_- ground-state band gives a measure of the total population of P excited states (P_-^* and P_+^*), whereas the population of P_-^* can only be monitored by its SE. Care must be taken in interpreting SE kinetics, since they are modulated by coherent nuclear motions and in particular the kinetics on the time scale of ~ 100 fs are strongly wavelength-dependent.³⁵ Upon direct excitation of P_- a pure delay of ~ 70 fs in the onset of SE is monitored at 920 nm and 90% of its maximum is reached after ~ 90 fs (Figure 4B). Upon excitation at 820 nm, 90% of the maximal signal at 920 nm is reached only after ~ 180 fs (Figure 4B), indicating that SE appears on the order of ~ 100 fs more slowly than upon excitation at 880 nm. Whereas directly fitting the kinetics with exponential functions is inadequate, a rough time range of the appearance of SE can be obtained by comparing the experimental 820 nm excitation kinetics and simulated convolutions of the 880 nm signal with an exponential rise (Figure 4B). This procedure indicates that upon excitation at 820 nm, a major part ($\sim 90\%$) of the population of P_-^* takes 50–100 fs. Together with the observation of direct excitation of P in $\sim 90\%$

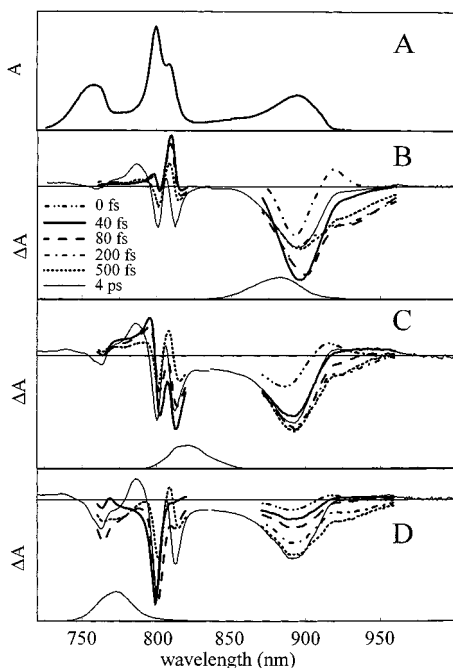


Figure 6. Ground-state (A) and transient (B–D) spectra at selected delay times of *R. sphaeroides* R26 RCs at 15 K. Maxima of the excitation pulses were at 880 nm (B), 820 nm (C), and 770 nm (D). The spectral profiles of the pump pulses are drawn at the bottom of each panel. The spectra in each panel were taken in two parts: one where the probe was compressed at ~ 800 nm and one where the probe was compressed at ~ 920 nm. The spectra of the two parts are normalized to the overlapping 800–860 nm spectral range at 4 ps. For the subpicosecond delay times, only the spectral region where the chirp was less than 15 fs is shown. For clarity, in the blue region only the 40, 80, and 500 fs and the 4 ps spectra are shown.

of the centers, we conclude that internal conversion from P_{+}^{*} to P_{-}^{*} takes 50–100 fs.

3.2.5. Spectral Evolution on the Picosecond Time Scale. After ~ 700 fs the spectral evolution is similar, but not identical, for all excitation conditions, consistent with the results of Lin et al.²² For narrow-band excitation. For instance, in the 10 ps spectra of Figure 3, small differences can be seen in the extent of the bleaching near 760 nm. Furthermore, after ~ 700 fs, the relative (with respect to 860 nm) amplitude of the signal at 920 nm is substantially lower upon excitation at 770 or 820 nm ($\sim 85\%$) than upon direct excitation of P_{-} at 880 nm (inset of Figure 3A, Figure 4B). This indicates that the decay of excited states to a state in which P is bleached (presumably P^{+}) does not necessarily occur via a pathway involving P_{-}^{*} , or in other words, that P_{-}^{*} is not always the precursor of charge separation.^{22–24}

3.3. *R. sphaeroides* R26 at 15 K. The band narrowing and enhanced spectral separation at cryogenic temperature (Figure 6) should in principle allow a more detailed interpretation of the transient spectra in terms of pathways of energy transfer. With this aim we conducted experiments at 15 K under otherwise the same experimental conditions as at RT. A comparison of the data obtained using 880,⁴⁶ 820, and 770 nm excitation is presented in Figures 6 (transient spectra), 7 (transient kinetics in the P_{-} absorption and P^{*} SE emission region), and 8 (transient kinetics in the B- and H-band region).

Following similar reasoning as above for the RT data, it can be seen that (a) upon excitation of H and B with 770 nm pulses, H^{*} decays in less than 100 fs to B^{*} and B^{*} decays in 200–300 fs concomitant with the appearance of P^{*} and (b) upon excitation of P_{+} with 820 nm pulses, internal conversion takes 50–100 fs. Thus, a general comparison of the spectral evolution at 15

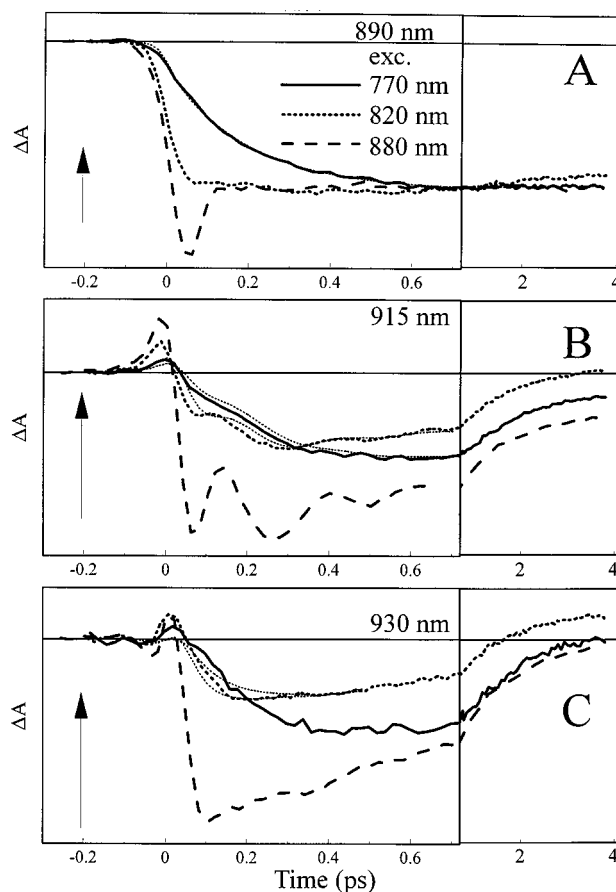


Figure 7. Kinetics of *R. sphaeroides* R26 RCs at 15 K at 890 nm (A), where bleaching of P is mainly monitored, and at 915 nm (B) and 930 nm (C), where P^{*} stimulated emission is monitored. Excitation is at 880 nm (---), 820 nm (···), and 770 nm (—). The kinetics are normalized to that at 890 nm, 0.7 ps. In panel A are also shown (···) a fit of the 770 nm data with a rise time of 210 fs and a decay time of 0.9 ps. In panels B and C are also shown (···) the respective experimental 880 nm excitation kinetics convoluted with rise times of 50 and 100 fs (B) and 75 fs (C) (all normalized to the respective 820 nm excitation data) and of 250 fs (B, normalized to the 770 nm excitation data). The vertical arrows in each panel represent identical absorption changes. Note the different time scales.

K and RT shows that the kinetics of downhill energy transfer are virtually temperature-independent. However, several of the spectral details not observed at RT allow a more refined interpretation, and furthermore, the question of vibrational coherence in the product states of energy transfer can be addressed because of the strong modulation of the kinetics by oscillatory features. Finally, at 15 K, the transient spectra on longer time scales display a strikingly stronger dependence on the excitation conditions than at RT. In the following we will describe the 15 K features yielding information additional to or differing from that at RT.

3.3.1. Nature of the P_{+}^{*} State. Upon excitation at 820 nm, $>90\%$ of the ground-state bleaching of P at 890 nm appears instantaneously (<20 fs) (Figures 6C and 7A), indicating that P_{+} and P_{-} are mainly excited. In the B-band region, initial bleachings centered at ~ 813 and ~ 802 nm, an induced absorption with a peak at ~ 796 nm and a zero-crossing at ~ 799 nm are observed (Figure 6C). We tentatively assign the initial bleaching at 813 nm to bleaching of the P_{+} band (following the assignment of Breton³⁶ for the 811 nm shoulder in the B band to P_{+}) and to P_{+}^{*} SE. The 813 nm bleaching mostly decays on the ~ 100 fs time scale (Figure 8C), presumably because of $P_{+}^{*} \rightarrow P_{-}^{*}$ internal conversion, as P_{-}^{*} SE rises on a similar time scale (parts B and C of Figure 7). The shiftlike

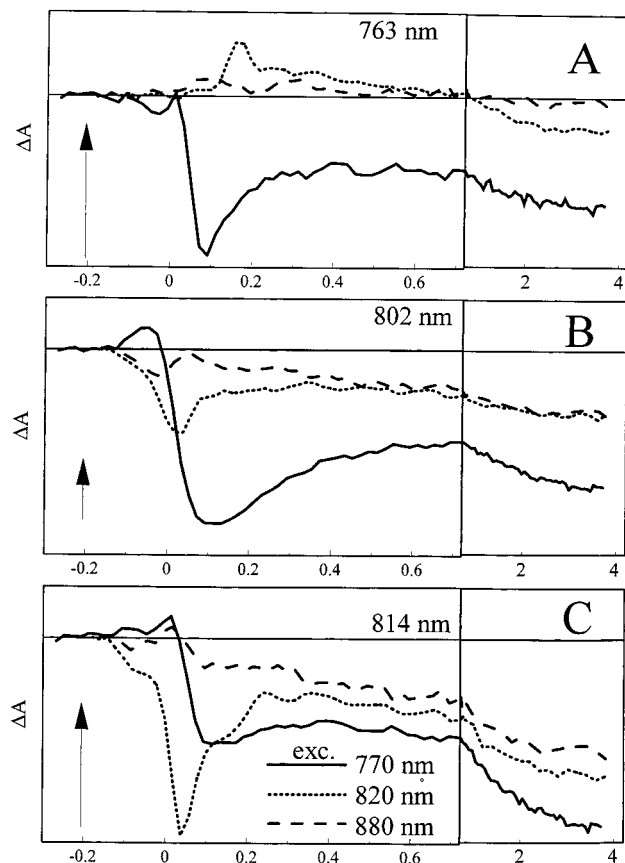


Figure 8. Kinetics of *R. sphaeroides* R26 RCs at 15 K at 763 nm (A), 802 nm (B), and 814 nm (C). Excitation is at 880 nm (---), 820 nm (···), and 770 nm (—). The kinetics are normalized as in Figure 6. The vertical arrows in each panel represent identical absorption changes. Note the different time scales.

feature around 799 nm (comprising the 796 nm induced absorption and 802 nm bleaching) also relaxes on this time scale, indicating that it is also associated with P_+^* . A possible interpretation of this shift is that P_+^* carries charge-transfer character (such as $P_L^+P_M^-$, $P_L^+B_L^-$, etc.), the electric field of which induces a Stark effect on the spectrum of B_L or B_M or both. If this is correct, this would imply that the charge-transfer character of P_+^* differs from that of P_-^* (shiftlike features in this region are weaker upon direct excitation in P_- ; see Figure 6B). The assignment of the shift to P_+^* rather than to B^* is consistent with the fact that it is not observed on the time scale of ~ 100 fs upon excitation at 770 nm, where B^* should be populated substantially.

A spectral deconvolution of the ground-state absorption spectrum (not shown) shows that the 820 nm pulse overlaps, to comparable extents, with the main 801 nm band (B) and with the 811 nm shoulder (P_+). The initial bleaching at ~ 802 nm observed upon excitation at 820 nm may therefore also reflect B^* . The decay pathway of this B^* is not clear; the $>90\%$ bleaching of P appearing in less than 20 fs (Figure 7A) indicates that little $B^* \rightarrow P^*$ transfer occurs in ~ 200 fs (the time scale for $B^* \rightarrow P^*$ found from the 770 nm excitation data). It therefore would seem that B^* , formed with 820 nm excitation, essentially decays by following pathways not involving P^* . B^* formed with 770 nm pulses appears to decay to P^* to a significant (though not full; see below) extent. The strong bleaching at ~ 800 nm observed in the tens of femtosecond time scale decays by $\sim 50\%$ in 200–300 fs with a concomitant appearance of P_- ground-state bleaching and P_-^* SE (Figures 6D, 7B, and 8). During the latter spectral evolution, the amplitude of the absorbance change at 890 and at 800 nm is

similar but of opposite sign (Figure 6D). The observed contribution of less than 10% of such an evolution to the bleaching of the P_- band upon excitation at 820 nm would thus imply that B is excited to less than 20% under these conditions. This would indicate that the contribution of P_+ to the B band is much larger than expected. The alternative possibility that coherent excitation of B^* and P_+^* by the broad 820 nm pulse is responsible for this discrepancy will be presented in the Discussion.

3.3.2. Vibrational Coherence. It is well-documented that direct excitation of P_- activates coherent low-frequency motions in P_-^* , which are detectable through the oscillatory modulation of the kinetics of P_-^* stimulated^{18,19} (see Figure 7B) and spontaneous²⁰ emission. An interesting question is to what extent such motions are also activated if P_-^* is populated from a higher-lying electronic state. In agreement with previous fluorescence experiments,¹⁵ Figure 7B shows that on the blue side of the SE band (915 nm) very similar oscillations (main frequency ≈ 130 cm^{-1}) are observed upon excitation of P_+ at 820 nm and of P_- at 880 nm. The relative amplitude (with respect to the amplitude of the kinetics with the same excitation conditions) of the former oscillations is ~ 2 times lower. The 820 nm excitation kinetics can be well simulated by convoluting the experimental 880 nm excitation kinetics with a rise time of 75 fs, indicating that this ratio corresponds well with that expected for a wave packet oscillating with a period of 250 fs (130 cm^{-1}) populated in ~ 75 fs (by internal conversion from P_+^* ; see above) instead of 30 fs (by a 880 nm pump pulse). Upon excitation at 770 nm, the amplitude of the oscillatory features is very strongly reduced, though yet discernible. The main features of the kinetics can be simulated (Figure 7B) in a way similar to that for the 820 nm excitation data, using a population time of 250 fs (time scale of $B^* \rightarrow P^*$ transfer; see above). A similar analysis can be made for the kinetics at the red side of the SE band, where the same oscillations appear in counterphase^{18,19} (not shown) and at RT, where the amplitude of the oscillations is lower.³⁵ Altogether these observations strongly suggest that the same coherent motions are activated in P_-^* whether it is populated by direct light absorption of P_- or indirectly by energy transfer.

The kinetics in the H- and B-band spectral region are also modulated by oscillatory features, both at cryogenic temperatures⁴⁷ and at RT.^{34,48} The complicated wavelength dependence of these features observed upon excitation at 880 nm will be characterized elsewhere. Here, we note that upon excitation at 820 nm, the kinetics in the 813 nm spectral region (Figure 8C) are strongly modulated by oscillatory features with a main frequency of ~ 250 cm^{-1} (period of ~ 130 fs), which can in principle be due to electronic or vibrational coherences. However, the fact that they persist for at least several hundred femtoseconds indicates that they do not reflect electronic coherence (which is lost more quickly; see section 3.1) and more generally are not related to oscillations involving the decaying excited state. Since strong 250 cm^{-1} features are not observed in this spectral region upon direct excitation of P_- (Figure 8C), it seems unlikely that they reflect vibrational motions on the product state (P_-^*) potential energy surface. We favor the remaining possibility that they reflect coherent nuclear motions in the ground state. We note that Jonas et al.¹³ have also observed oscillations in their one-color pump–probe experiments with a similar frequency (227 cm^{-1}) but with a decay time of 90 fs. This apparent much faster decay time may be due to a greater sensitivity to frequency inhomogeneity in their case, where the probe pulse is not spectrally resolved.

3.3.3. Deviations from a Linear Energy-Transfer Scheme.

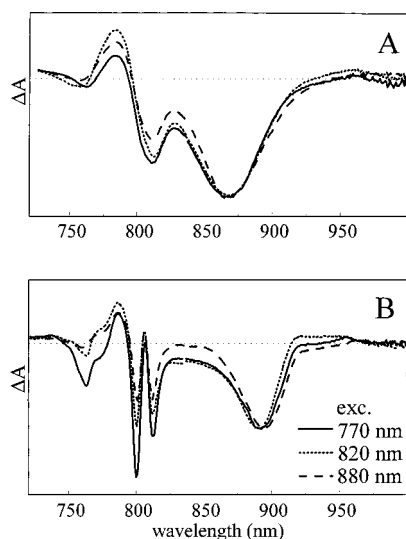
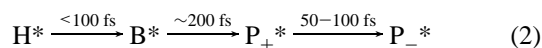


Figure 9. Transient spectra of *R. sphaeroides* R26 RCs at RT and 10 ps (A) and at 15 K and 4 ps (B) upon excitation at different wavelengths. The spectra are normalized at 870 nm (A, taken from Figure 3) and 890 nm (B, taken from Figure 6).

Altogether, the simplest scheme that describes the ensemble of the fast (<300 fs) phases that we resolve is



These time scales apply both at room temperature and at 15 K.

Such a scheme would suggest that after a few hundred femtoseconds, P_-^* is fully populated irrespective of the excitation conditions. For all excitation conditions it would then be expected that electron transfer, taking place on the time scale of picoseconds, occurs from the same precursor state P_-^* and follows the same pathways as those with similar transient spectra. In agreement with previous work,²²⁻²⁴ we observed that this is clearly not the case (Figure 9), especially at 15 K and RT, indicating that this scheme accounts only for part of the decay of higher-lying excited states.

In more detail, the 4 ps, 15 K transient features at 813, 800, 785, and 763 nm are all similar in shape but vary significantly in relative amplitudes with the three excitation conditions. Upon excitation at 820 nm they are larger (with respect to the P_- bleaching) by 20–35% for the first three features and by ~100% for the 763 nm bleaching compared to the corresponding features upon excitation at 880 nm. Upon 770 nm excitation, the bleachings at 813 nm (~50%), 800 nm (~100%), and especially 763 nm (at least a factor 4) are even much higher. Whereas the 820/880 nm excitation differences in the amplitudes of the 813, 800, and 785 nm features might be related to the normalization with respect to the P_- band,⁴⁹ the differences of the other features are far too strong to be ascribed to the normalization procedure. Thus, the relative population of electronic states measured after several picoseconds is remarkably dependent on the excitation wavelength. For 770 nm excitation, the strong bleachings at 763 and 800 nm indicate that this population includes H_L (rather than H_M , which is thought to absorb more at the blue side of the H band¹) and B excited states or radicals. One possibility is that a fraction of H_L^* and/or B^* formed by the pump pulse is incapable of downhill energy transfer on the picosecond time scale. Another possibility is that radical pairs such as P^+B^- or $P^+H_L^-$ are formed.²⁴ Since uphill energy transfer from B^* or P_+^* to H^* cannot occur to any significant extent ($\Delta E \gg kT$), the strong 763 nm bleaching at 4 ps upon excitation at 820 and 770 nm

(here, the bleaching grows on the time scale of picoseconds after its initial decay in <100 fs) cannot be due to H^* . Thus, this bleaching must be ascribed to a Bpheo radical (most likely H_L^-). Upon excitation at 880 nm, the bleaching of the H band at 763 nm is nearly completed at 4 ps (not shown). This indicates that the spectral difference is not due to a faster $P^+H_L^-$ formation upon excitation of different subpopulations of RCs, in agreement with the results of Peloquin et al.⁴²

The number of excitations that decay via pathways not including P^* may be crudely estimated. Upon 770 nm excitation at 15 K, it is probably as high as ~50%. This estimate is based on the observation that the strong bleaching at ~800 nm decays by ~50% in 200–300 fs with a concomitant appearance of P_- ground-state bleaching and P_-^* SE (Figures 6D, 7B, and 8).⁴¹ Likewise, we note that upon 820 nm excitation at 15 K, the ratio of P_-^* SE and P_- ground-state bleaching is lower by ~50% than upon excitation at 880 nm (Figures 6 and 7), indicating that, under these excitation conditions, P_+^* decays to a state other than P_-^* by somewhat less than 50%.⁴⁹ These values are very similar to those previously reported for the YM210W mutant at 77 K under narrow-band excitation centered at 799 nm.²⁴ Similar considerations for the RT data lead to values that are on the order of 10–20%, in agreement with the results of ref 22.

3.4. *Rps. viridis*. RCs of *Rps. viridis* bind the more red-absorbing cofactors Bchl *b* and Bpheo *b* where RCs of *R. sphaeroides* bind Bchl *a* and Bpheo *a*. Whereas the arrangement of the cofactors is very similar in both species,⁵¹⁻⁵³ in *Rps. viridis* the P_- band is located further (by ~700 cm^{-1} at low temperature) below the B and the P_+ bands than in *R. sphaeroides*. As a consequence, the spectral overlap of B^* emission and P_- absorption is much less in *Rps. viridis* than in *R. sphaeroides*. If direct $B^* \rightarrow P_-^*$ energy transfer were to occur in *R. sphaeroides* RCs,¹⁷ such a process would be expected to occur much more slowly in *Rps. viridis*.

To investigate this, we performed additional experiments on *Rps. viridis* RCs, upon excitation at 770 nm where H_M is preferentially excited, at 820 nm where one expects to excite preferentially H_L and B, and at 940 nm directly into the P_- band.⁵⁴ Many of the general features found for excitation in the H and B bands of *R. sphaeroides* were observed, including excitation wavelength-dependent spectra on the picosecond time scale. Here, we show only kinetics in the P_- band region obtained with the different excitation conditions (Figure 10). The P_- band bleaching clearly appears within a few hundred femtoseconds upon excitation in the H and B bands. Figure 10 shows best fits with time constants of 170 fs (RT and 15 K) for excitation at 770 nm and 90 fs (RT) and 80 fs (15 K) for excitation at 820 nm. The SE signal (within our spectral window only for the RT data) appears somewhat slower than the signal for the P_- ground-state bleaching but is also completed within a few hundred femtoseconds. These results show that in a large fraction of the centers, P_-^* is formed on a similar time scale, and possibly even somewhat faster, than in *R. sphaeroides*. As explained above, it is therefore highly unlikely that energy is transferred directly from B^* to P_-^* .

The results for *Rps. viridis* are consistent with a similar scheme derived for *R. sphaeroides*. The kinetics are also virtually temperature-independent. The observed rise times would indicate that $B^* \rightarrow P_+^*$ occurs in ~90 fs and $H_L^* \rightarrow P_+^*$, probably via B^* , in ~170 fs. These values are somewhat faster than the value of ~200 fs deduced for *R. sphaeroides*. We stress, however, that the highly congested bands in the B- and H-band regions complicate a detailed analysis.

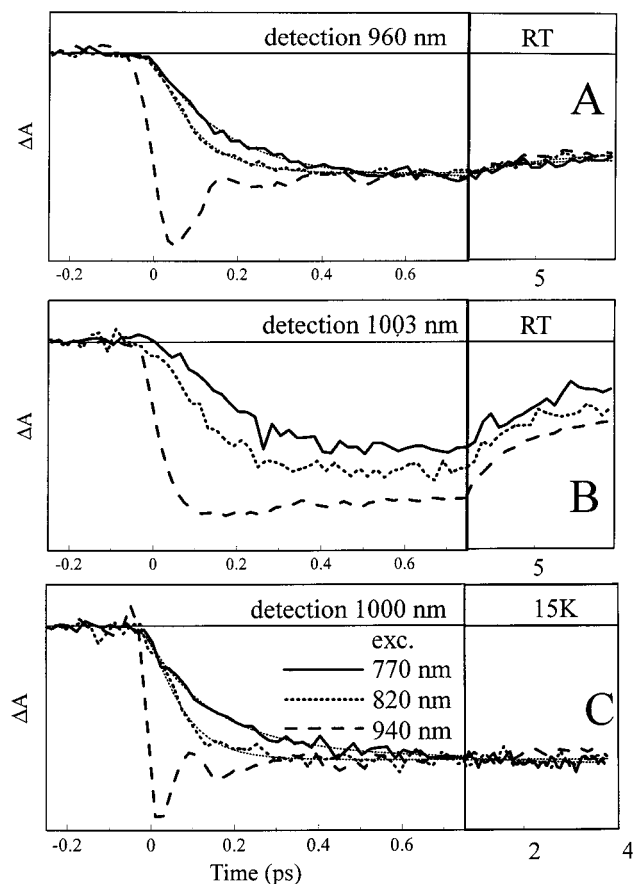
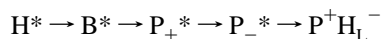


Figure 10. Kinetics of *Rps. viridis* RCs at RT (A, B) and 15 K (C). Excitation at 940 nm (---), 820 nm (···), and 770 nm (—). Superimposed on the 820 and 770 nm excitation kinetics reflecting the bleaching of the P_- band (A, C) are exponential fits (···) as described in the text. The data in parts A and C are normalized to data at 0.7 ps and those in part B are scaled as in part A. Note the different time scales.

4. Discussion

As discussed by Lin et al.,²² monitoring the full spectral evolution in the Q_Y region of the bacteriochlorin pigments reveals excitation-wavelength-dependent features on the picosecond time domain that are not apparent in normalized single-wavelength transients. When monitored with a 30 fs time resolution, as in the present study, a very complex spectral evolution is observed both on the ~ 100 fs time scale and on the picosecond time scale that cannot be fully described in terms of a simple exponential model. At both RT and 15 K, part of the spectral evolution can be described in terms of the scheme



which will be discussed first. Alternative pathways of energy and electron transfer, which are especially apparent at low temperature, will be discussed subsequently.

4.1. Temperature Dependence of Downhill Energy Transfer. The time scales we found for the downhill energy-transfer processes are highly temperature-independent, both for RCs from *R. sphaeroides* R26 (in agreement with results from previous fluorescence experiments^{15,16}) and from *Rps. viridis*. In electronic energy transfer, the temperature dependence is expected to be mostly related to changes (narrowing upon cooling) in the emission and absorption spectra of the donor and acceptor, respectively.⁵⁵ In particular, if the spectral overlap depends strongly on the tail of the bands, a strong temperature dependence can be expected. The absence of any sizable effects thus indicates that the overlap is near the optimum, in general

agreement with the high speed of the transfer. For $B^* \rightarrow P_+^*$ transfer in *R. sphaeroides*, this is in agreement with the notion that the difference in the maxima of the B and P_+ transitions (~ 10 nm, 160 cm^{-1}) corresponds roughly to the Stokes shift of Bchl *a* (190 cm^{-1} in ether⁵⁶). For $H^* \rightarrow B^*$ transfer this correspondence seems somewhat less optimal (~ 640 and 260 cm^{-1} ⁵⁶); however, we note that the emission spectra of H^* and B^* in the RC are essentially unknown.⁵⁷

The observed temperature insensitivity facilitates comparison with other data and justifies, for many aspects, a common discussion of the results at all temperatures.

4.2. Energy Transfer toward P_-^* . It has been reported previously that the rise times of the spontaneous emission of wild-type *R. sphaeroides* RCs at 85 K upon excitation centered at 825, 804, and 759 nm is ~ 80 , 150, and 250 fs, respectively,¹⁵ and that of SE in *R. sphaeroides* R26 at RT upon excitation centered at 810 nm is ~ 110 fs.¹⁷ Our results indicating that the P_-^* SE rise, which is not instantaneous upon excitation in P_- ¹⁹ and is convoluted with a rise time of 50–100 fs upon excitation at 820 nm and ~ 200 fs upon excitation at 770 nm, are in good agreement with these observations. An important observation is that excitation at 820 nm instantaneously (< 20 fs) leads to bleaching of the P_- band.⁵⁸ Together with the P_-^* emission rise time this provides a time of 50–100 fs for $P_+^* \rightarrow P_-^*$ internal conversion. In this reasoning it is assumed that the nuclear dynamics modulating P_-^* SE are similar for direct excitation of P_- and for internal conversion from P_-^* , as will be discussed in section 4.2.4.

We note that in a scheme where P_+^* also decays to states other than P_-^* , as will be discussed in section 4.3, the *intrinsic* internal conversion time may be somewhat longer.

4.2.1. Population of B^* upon Excitation at 820 nm? The distribution of excited states initially populated by the 820 nm pulse thus seems to consist mainly of P_+^* and P_-^* . This result is somewhat surprising, since the P_+ transition is generally thought to contribute only a minor fraction (10–20%) to the total 800 nm band, as discussed in great detail by Haran et al.¹⁷ In brief, such numbers have been estimated from exciton calculations based on the X-ray structure incorporating the dimer P only¹⁷ or the ensemble of bacteriochlorins.⁶⁰ These estimates are in agreement with spectroscopic data showing that the surface of the B-band region does not decrease by more than $\sim 10\%$ upon oxidation of P.^{36,61}

In a Gaussian deconvolution of the 15 K absorption spectrum (Figure 6A), even when assigning the entire shoulder ($\sim 1/3$ of the total surface of the B/ P_+ band) at 811 nm to P_+ , we found that the overlap of this band with the 820 nm pump pulse was of the same magnitude as that of the band at 801 nm. In addition, $\sim 20\%$ of the pulse overlaps with the high-energy tail of P_- .⁴⁹ Altogether, it would seem that the excited states created by the 820 nm pulse contain at least 40% B^* . To explain that the bleaching of P_- appears instantaneously for $> 90\%$, in principle four possibilities can be envisaged: (1) $B^* \rightarrow P_+^*$ energy transfer occurs in less than 20 fs; (2) $B^* \rightarrow P_+^*$ energy transfer does not occur in the investigated time range; (3) the contribution of P_+ to the 800 nm band is much larger than assumed; (4) B and P_+ are coherently excited by the pump pulse. The first possibility seems unlikely, since (a) < 20 fs for energy transfer would be faster than the estimated electronic dephasing time (~ 80 fs) at 15 K and (b) this is inconsistent with the results obtained upon excitation at 770 nm and with those by more selective excitation in the B band.^{22,62} The second possibility is also inconsistent with the results obtained upon excitation at 770 nm if more than 20% of the excited states formed consist of B^* , as discussed in section 3.3.1. The third possibility, that

essentially P_+ (and P_- to a minor extent) overlaps with the 820 nm pulse, cannot be entirely excluded. However, as discussed above, it is inconsistent with the common view of the composition of the B band. In addition, we note that Stanley et al.¹⁵ found that the anisotropy of P_-^* fluorescence (which appeared delayed with respect to direct excitation of P_-) upon impulsive excitation at 825 nm was >0.3 , whereas negative values are expected for pure excitation of P_+ . This also supports the idea that in our case, where the excitation pulse extends more to the blue, B must be excited to a significant extent.

In the fourth possibility that we propose, excitation of B and P_+ by the broad band pump pulse leads to population of a coherent superposition of the electronic eigenstates and bleaching of both B and P_+ and hence of P_- . In this mechanism, it is expected that the population subsequently oscillates between B^* and P_+^* with a frequency corresponding, for near-degenerate states, to the interaction between the two states.⁶³ In our case electronic dephasing (in ~ 80 fs at 15 K and possibly faster at RT; see section 3.1) will strongly damp these oscillations and localize the excitation, presumably mainly in the lower-lying state P_+^* .⁶⁴ $P_+^* \rightarrow P_-^*$ internal conversion then takes place in 50–100 fs.

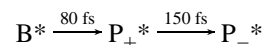
A lower limit of ~ 100 cm⁻¹ for the interaction energy can be estimated by assuming critical damping of the oscillations at low temperature. Therefore, the possibility of coherently exciting B and P_+ suggests substantial coupling between P and B, such as advanced in some theoretical studies^{38,39} and also suggested from the strong perturbations in the B band observed upon excitation in the P_- band.²¹ A mechanism of $B^* \rightarrow P_+^*$ energy transfer with an "internal conversion" character has been put forward by both Haran et al.¹⁷ and by Jonas et al.¹³ in the context of different pump–probe experiments in which *the pump pulse overlapped with both B and P_+ bands*. We stress that the mechanism only applies when B and P_+ are coherently excited, since $B^* \rightarrow P_-^*$ transfer appears much more slowly (~ 200 fs) when B^* is populated by using a 770 nm pulse, which has negligible overlap with P_+ .

More generally, the result that P_- strongly bleaches instantaneously upon excitation at 820 nm demonstrates that P transitions significantly contribute to the absorption in the B-band region. This is consistent with proposals from several experimental^{17,36,65} and theoretical^{38,39,60} studies. Our results do not justify the ignoring of the contributions of P to the B band in the detailed Gaussian-deconvolution analysis of the RC spectrum by Steffen et al.⁶¹

4.2.2. $H^* \rightarrow B^*$ Transfer. Consistent with the observations of Lin et al.,²² which were obtained with 150 fs pulses, we found that H^* at least partly decays in less than 100 fs undoubtedly to B^* and not directly to P^* , which appears only in ~ 200 fs. The latter observation of delayed P^* formation upon excitation of H and B contrasts with early single-wavelength kinetics from this laboratory with 150 fs pulses.⁸ These measurements probably have been biased by relatively high pulse intensities for which energy-transfer experiments are very sensitive^{7,8,13} and by the uncertainty in the zero-of-time. We note that a transfer time of ~ 100 fs for $H^* \rightarrow B^*$ appears consistent with a Förster weak coupling mechanism.^{10,15}

4.2.3. Pathway of $B^* \rightarrow P_-^*$ Transfer. The 50–100 fs $P_+^* \rightarrow P_-^*$ internal conversion time, deduced from the rise in the emission upon excitation at 820 nm observed by us and by others,¹⁵ is much faster than the ~ 200 fs $B^* \rightarrow P_-^*$ transfer observed when B^* is populated using a pulse that does not overlap the P_+ band. If the latter transfer passes via P_+^* , as will be discussed below, then $B^* \rightarrow P_+^*$ is the rate-limiting step in this process. The resulting scheme (eq 2), based on our

multicolor experiments, proposes the same $B^* \rightarrow P_-^*$ decay route as deduced from the model of the polarized one-color experiments by Jonas et al.,¹³



but with roughly interchanged time scales for both processes. Whereas the kinetic data in the B-band region appear to be in agreement, this difference probably arises from (a) their analysis of the data in an exponential model and ignoring decay routes other than to P_-^* and (b) our finding that a fundamentally different situation applies when B^* is populated by a broad pulse overlapping with the P_+ band than when it is populated by a more blue pulse, either directly or by energy transfer from H^* .

Haran et al.,¹⁷ challenging the validity of previous calculations by Jean et al.,¹⁰ have argued that the high-energy tail of the P_- band allows enough spectral overlap with B^* emission to envisage direct $B^* \rightarrow P_-^*$ transfer in ~ 100 fs via a weak coupling Förster mechanism. This was contested by Stanley et al.¹⁵ based on the temperature independence of the energy transfer. Our present results also argue against such a mechanism. First, the apparent small difference in the rise kinetics in the P_- absorption and emission bands at RT (Figure 4) indicates that P_+^* is an intermediate in $B^* \rightarrow P_-^*$ transfer. Second, our, as well as other,⁴² low-temperature measurements show that the P_- high-energy tail is mainly due to inhomogeneous broadening, since it does not bleach upon excitation at 880 nm (Figure 9). This implies that the overlap argument is valid only for a small fraction of the centers. Finally, $B^* \rightarrow P_-^*$ was found to occur on the same time scale as in *Rps. viridis*, where the energy gap between B^* and P_-^* is much larger (and the B^* -emission/ P_- -absorption spectral overlap presumably much smaller) than in *R. sphaeroides*.

The above arguments that the energy transfer is insensitive to B^* -emission/ P_- -absorption spectral overlap indicate that a hypothetical direct $B^* \rightarrow P_-^*$ transfer would occur neither in the weak coupling¹¹ nor in the electronic exchange⁶⁶ limit of electronic energy transfer, since in both cases the rate would be proportional to the (somewhat differently weighted⁶⁷) spectral overlap. This further justifies the analysis in terms of $B^* \rightarrow P_+^*$ energy transfer and subsequent internal conversion to P_-^* made throughout this paper. The ~ 200 fs $B^* \rightarrow P_+^*$ transfer is an order of magnitude faster than the 2–3 ps calculated for this process using weak coupling Förster theory.¹⁰ Closely following the discussion by Jonas et al.,¹³ it is actually nearer to the "interaction time" of ~ 120 fs estimated for the strong coupling limit of Förster theory. The suggestion that P_+ and B can be coherently excited, as discussed above, is also consistent with a strong coupling between those states. Altogether, the processes of electronic dephasing, $B^* \rightarrow P_+^*$ energy transfer, P_+^* internal conversion, and coherent motion out of the Franck–Condon region in P_-^* ¹⁹ all take place in a similar time range. Whereas our present analysis is based on a minimal interpretation of the data in terms of these processes, extensive theoretical modeling will be needed for a complete description of these processes and their interplay.

4.2.4. Vibrational Coherence in P_-^* . The equilibrium configuration of the RC in the P_-^* state is displaced with respect to the ground state. Therefore, when P_-^* is populated directly from the ground state, nuclear motions are brought about. They have mainly a low-frequency (<200 cm⁻¹) nature for a variety of modes, including a prominent set of modes near ~ 130 cm⁻¹.^{19,35,43,50,68} These motions modulate the femtosecond emission kinetics,^{18–20} are underdamped, and maintain their phase on the time scale of electron transfer.^{19,20,35} In agreement

with results from earlier fluorescence experiments,¹⁵ we found that oscillations also modulate the P_{-}^{*} SE kinetics upon excitation in the other Q_Y transitions of the RC. Comparison of the properties of these oscillations observed under the various excitation conditions shows that they reflect motions along the same modes on the P_{-}^{*} potential energy surface, activated upon transfer from higher-lying electronic states. This indicates that the nuclear configuration is not much modified prior to energy transfer to P_{-}^{*} , in general agreement with the notion that coupling to low-frequency modes of the B and H transitions is weaker than that of P.^{43–45}

In intact, antenna-containing membranes, the population of antenna excited states will probably modify the RC configuration to an even lesser extent than H^{*} , B^{*} , or P_{+}^{*} . Therefore, the conclusion that the same coherent motions are activated whether P_{-}^{*} is populated directly or indirectly by intra-RC energy transfer can probably be extended to energy transfer from the antenna. Whereas the functional role of the P_{-}^{*} coherent motions is not yet established, it thus seems likely that they will also occur during electron transfer in intact systems.

4.3. Other Decay Routes. Whereas the spectral changes on the ~ 100 fs time scale upon excitation in the B and H band can be understood in terms of energy transfer toward P_{-}^{*} , summarized in eq 2, spectral differences are observed under the different excitation conditions after completion of these phases. This confirms that the initially created excited states also decay toward electronic states other than P_{-}^{*} . At RT, spectral differences in the B and H bands were observed up to our longest delay time of 10 ps. Similar data, obtained with spectrally narrower and longer excitation pulses, were previously reported by Lin et al.²² These authors demonstrated that the ensemble of centers relaxes to an almost excitation-independent distribution of electronic states (presumably mostly $P^{+}H_L^{-}$) after 25 ps. They proposed an interesting model of electron transfer in which the excited states populated after the fast energy-transfer phases are vibrationally hot and relax via different pathways on an adiabatic potential energy surface to an electronic state with predominant $P^{+}H_L^{-}$ character. It was proposed that P^{*} was not a necessary intermediate and that radical pairs such as $P^{+}H_L^{-}$ and $B_L^{+}H_L^{-}$ could be populated from B^{*} and H^{*} . A report by van Brederode et al.²³ on 77 K fluorescence excitation spectra of the YM210W mutant in which P_{-}^{*} decays very slowly supports the possibility of electron transfer from precursors other than P_{-}^{*} and suggests these precursors to be B_L^{*} and H_L^{*} . Further work by these authors²⁴ using multicolor femtosecond spectroscopy upon excitation in the B band confirmed these results and was analyzed in terms of an exponential model suggesting that a mixture of $P^{+}B_L^{-}$ and $B_L^{+}H_L^{-}$ was formed prior to $P^{+}H_L^{-}$. In this mutant, at 77 K, the yield of the electron transfer via those alternative pathways was found to be $\sim 50\%$,^{23,24} substantially higher than the value of $\sim 15\%$ reported for wild-type RCs at RT.²²

The data presented here further support the existence of electron-transfer pathways bypassing P_{-}^{*} and directly show in the same system that they are more important at low temperature: (a) the excitation-wavelength dependence of the emission yield is much more dramatic than at RT and (b) at delay times where the formation of the primary photoproduct (presumably $P^{+}H_L^{-}$) upon direct population of P_{-}^{*} has been nearly completed, excitation of B/P₊ and especially H yields larger amounts of photoproducts that apparently do not involve P. These alternative photoproducts may in principle consist of (a) radical pair states and (b) partially, but not exclusively (see section 3.3.4.), excited states (H^{*} , B^{*}). The latter possibility would imply remarkably strong inhomogeneity in the transfer times

(for instance, such inhomogeneity is not expected for energy transfer along the L and M branches¹⁵) and furthermore would be inconsistent with hole-burning results.⁶⁸ Thus, whereas measurements of H^{*} , B^{*} , and P_{+}^{*} by femtosecond spontaneous emission are needed to directly address this issue, it seems unlikely that substantial H^{*} and B^{*} states are still present on the picosecond time scale, and we favor the possibility that radical pairs other than $P^{+}H_L^{-}$ are formed.

In the 770 nm excitation, 15 K, 4 ps transient spectra (Figure 9), the two bleachings that are predominantly enhanced with respect to excitation at 880 nm are centered at 763 nm (H_L) and 800 nm (B). In principle, it is possible that these two features are related to two different populations of radical states. For the 800 nm bleaching, these could involve $P^{+}B^{-}$ radicals.²⁴ However, for the 763 nm bleaching, these cannot involve the state $P^{+}H_L^{-}$ (this would yield the same spectrum as upon excitation at 880 nm), and other radical states not involving B seem unlikely. Therefore, and because the 763 and 800 nm bleachings appear in approximately stoichiometric amounts, the most likely candidate for the additional photoproduct formed on the picosecond time scale is $B^{+}H_L^{-}$.⁶⁹ In this proposal, the oxidized Bchl is most likely B_L located close to H_L . This would also be expected if the alternative route is generated mainly from excitations on the L-side pigments, as has been suggested to occur for the YM210W mutant.²³ The present results do not allow a clear distinction between the L and M branches. However, the relatively strong excitation of H_L (over H_M) with the 770 nm pulse is in agreement with this idea.

As mentioned above, for the case of 77 K B band excitation in a mutant RC, van Brederode et al.²⁴ also proposed that $B^{+}H_L^{-}$ is formed as an intermediate. In this case analysis of the B and P band spectral evolution returned a value of 14% for the yield of routes involving this species, much less than the $\sim 50\%$ that we estimate for wild-type RCs under 770 nm excitation at 15 K, and accordingly, we observe a much stronger bleaching of H_L after a few picoseconds. Assuming both assignments to $B^{+}H_L^{-}$ are correct, one might speculate that the difference is due to the preferential excitation of H in our case, suggesting that H^{*} may act as a direct precursor for this state. In very recent room temperature work of Jackson et al.⁷¹ on a mutant devoid of P, the trend in the difference of excitation in B (no $B^{+}H^{-}$ formed) and H (a small amount of other photoproduct, possibly $B^{+}H^{-}$, formed) is generally consistent with this suggestion. On the other hand, more generally, the absence of substantial electron transfer in this mutant argues against the possibility of $B^{+}H^{-}$ without involvement of P. However, in the comparison of these three studies (refs 24, 71, and our work), differences in (a) the electronic structure of the mutants and wild-type and (b) the temperature will also be important.

For the primary photoproduct formed upon excitation in the P_{-} band, generally ascribed to $P^{+}H_L^{-}$, the ratio of the apparent bleachings of the Q_Y bands of H_L and P is much lower (possibly as much as 10 times) than the ratio of the corresponding ground-state bands. Possible origins for this anomaly^{1,22,72} are that this state also carries substantial $P^{+}B_L^{-}$ character (but this is not supported by the spectrum in the anion bands¹ and in the Bpheo Q_X bands⁷³), substantial intensity borrowing between strongly coupled transitions of the hexachromophore system, or compensating effects due to induced radical absorption bands and especially to the blue shift of the B bands. B ground-state band shifts are expected to contribute much less to the transient spectrum of $B_L^{+}H_L^{-}$ (B_L is bleached and thus cannot shift; B_M is located relatively far from the radical pair) than to that of $P^{+}H_L^{-}$. This reasoning supports the suggestion that the strong bleaching of H_L observed in the 770 nm excitation (and to a

less extent, 820 nm excitation) photoproduct can be assigned to $B_L^+H_L^-$ and further would indicate that the nonstoichiometric bleaching of the $P^+H_L^-$ spectrum is mainly due to B-band shifts. It is interesting to note that the state $B_L^+H_L^-$ has been invoked previously as a possible intermediate in $P^* \rightarrow P^+H_L^-$ electron transfer^{74–76} and that it has been stressed that the state is coupled much more strongly to B^* and H^* than to P^* .⁷⁶ Our and other²⁴ results indeed suggest the light-induced formation of this state but not in the context of a necessary precursor for the state $P^+H_L^-$. If $P^+H_L^-$ would be formed from the putative $B_L^+H_L^-$ state, one expects to observe an additional bleaching of P_- . This is not observed on the time scale of 4 ps (Figure 7A). Assuming a single-exponential process, we estimate from our present limited data that it would take on the order of 100 ps or more, but it cannot be excluded that recombination to the ground state is more efficient. Experiments on longer time scales are required to investigate this point.

The photoproduct observed after 4 ps upon excitation at 820 nm at 15 K contains much more (but not exclusively) $P^+H_L^-$ than upon excitation at 770 nm (Figure 9). However, the reduced SE yield (Figures 6 and 7) indicates that P_-^* is a precursor for this state for only ~50% and that charge separation thus occurs for a substantial part from P_+^* or B^* directly. Intriguingly, upon 770 nm excitation at 15 K, within the fraction of excitations that lead to bleaching of P after 4 ps, the yield of P_-^* is substantially higher than upon excitation at 820 nm (Figures 6 and 7). This observation might be related either to the proposed coherent excitation at 820 nm or to more complicated parallel pathways of energy transfer. Experiments extended to longer time scales and other spectral regions, and possibly using spectrally more selective (and thus longer) excitation pulses, will be needed to further map out the possible pathways of excitation and electron transfer. At low temperature, these searches are facilitated not only by the better spectral separation but also apparently by “alternative” photoproducts that remain present to larger extent on a time scale where $P^+H_L^-$ formation upon direct excitation of P_- is completed. In the model proposed by Lin et al.,²² the latter feature might be due to the presence of multiple valleys in the adiabatic potential energy surface, which are not accessible when the excitation occurs into P_- .

5. Concluding Remarks

Our results represent a spectrally resolved characterization, with 30 fs time resolution, of the energy transfer and internal conversion processes occurring upon excitation in RC transitions at energies higher than that of P_- . This approach helps to disentangle the processes of electronic dephasing, energy transfer, internal conversion, and nuclear motion, all taking place on a time scale of ~100 fs. A direct result is that internal conversion from the upper to the higher exciton level of P^* takes 50–100 fs. Furthermore, our analysis suggests that P_+ and B can be coherently excited. This supports the evidence for strong coupling between P_+^* and B^* , a result that bears on our understanding of the electronic structure of the cofactor system.

We confirm that relaxation to the lowest excited-state P_-^* prior to charge separation is not complete.^{22,24} We found that this is especially the case at low temperature. Whereas it is a question of whether pathways not involving P^* are functionally relevant (energy transfer from the antenna to the RC is thought to occur from excited states approximately isoenergetic with P^* ⁷⁷), the concept of multiple pathways may also be applicable to electron transfer starting from P^* .

Acknowledgment. We thank Marion van Brederode, Simone Vulto, and Neal Woodbury for providing us with preprints of their work prior to publication. M.H.V. is supported by CNRS.

References and Notes

- (1) Kirmaier, C.; Holten, D. *Photosynth. Res.* **1987**, *13*, 225–260.
- (2) Zinth, W.; Kaiser, W. In *The Photosynthetic Reaction Center*; Deisenhofer, J., Norris, J. R., Eds.; Academic Press: San Diego, 1993; Vol. II, pp 71–88.
- (3) Kirmaier, C.; Holten, D. In *The Photosynthetic Reaction Center*; Deisenhofer, J., Norris, J. R., Eds.; Academic Press: San Diego, 1993; Vol. II, pp 49–70.
- (4) Martin, J.-L.; Breton, J.; Hoff, A. J.; Migus, A.; Antonetti, A. *Proc. Natl. Acad. Sci. U.S.A.* **1986**, *83*, 957–961.
- (5) Woodbury, N. W.; Becker, M.; Middendorf, D.; Parson, W. W. *Biochemistry* **1985**, *24*, 7516–7521.
- (6) Fleming, G. R.; Martin, J.-L.; Breton, J. *Nature* **1988**, *333*, 190–192.
- (7) Breton, J.; Martin, J.-L.; Migus, A.; Antonetti, A.; Orszag, A. *Proc. Natl. Acad. Sci. U.S.A.* **1986**, *83*, 5121–5125.
- (8) Breton, J.; Martin, J.-L.; Petrich, J.; Migus, A.; Antonetti, A. *FEBS Lett.* **1986**, *209*, 37–43.
- (9) Breton, J.; Martin, J.-L.; Fleming, G. R.; Lambry, J.-C. *Biochemistry* **1988**, *27*, 8276–8284.
- (10) Jean, J. M.; Chan, C.-K.; Fleming, G. R. *Isr. J. Chem.* **1988**, *28*, 169–175.
- (11) Förster, T. *Ann. Phys. (Leipzig)* **1948**, *2*, 55–75.
- (12) Jia, Y.; Jonas, D. M.; Joo, T.; Nagasawa, Y.; Lang, M. J.; Fleming, G. R. *J. Phys. Chem.* **1995**, *99*, 6263–6266.
- (13) Jonas, D. M.; Lang, M. J.; Nagasawa, Y.; Joo, T.; Fleming, G. R. *J. Phys. Chem.* **1996**, *100*, 12660–12673.
- (14) Du, M.; Rosenthal, S. J.; Xie, X.; DiMaggio, T. J.; Schmidt, M.; Hanson, D. K.; Schiffer, M.; Norris, J. R.; Fleming, G. R. *Proc. Natl. Acad. Sci. U.S.A.* **1992**, *89*, 8517–8521.
- (15) Stanley, R. J.; King, B.; Boxer, S. G. *J. Phys. Chem.* **1996**, *100*, 12052–12059.
- (16) Jonas, D. M.; Lang, M. J.; Nagasawa, Y.; Bradforth, S. E.; Dikshit, S. N.; Jimenez, R.; Joo, T.; Fleming, G. R. In *The Reaction Center of Photosynthetic Bacteria, Structure and Dynamics*; Michel-Beyerle, M. E., Ed.; Springer: Berlin, 1995; pp 187–198.
- (17) Haran, G.; Wynne, K.; Moser, C. C.; Dutton, P. L.; Hochstrasser, R. M. *J. Phys. Chem.* **1996**, *100*, 5562–5569.
- (18) Vos, M. H.; Rappaport, F.; Lambry, J.-C.; Breton, J.; Martin, J.-L. *Nature* **1993**, *363*, 320–325.
- (19) Vos, M. H.; Jones, M. R.; Hunter, C. N.; Breton, J.; Lambry, J.-C.; Martin, J.-L. *Biochemistry* **1994**, *33*, 6750–6757.
- (20) Stanley, R. J.; Boxer, S. G. *J. Phys. Chem.* **1995**, *99*, 859–863.
- (21) Vos, M. H.; Lambry, J.-C.; Robles, S. J.; Youvan, D. G.; Breton, J.; Martin, J.-L. *Proc. Natl. Acad. Sci. U.S.A.* **1992**, *89*, 613–617.
- (22) Lin, S.; Taguchi, A. K. W.; Woodbury, N. W. *J. Phys. Chem.* **1996**, *100*, 17067–17078.
- (23) van Brederode, M. E.; Jones, M. R.; van Grondelle, R. *Chem. Phys. Lett.* **1997**, *268*, 143–149.
- (24) van Brederode, M. E.; Jones, M. R.; van Mourik, F.; van Stokkum, I. H. M.; van Grondelle, R. *Biochemistry* **1997**, *36*, 6855–6861.
- (25) Breton, J. *Biochim. Biophys. Acta* **1985**, *810*, 235–245.
- (26) Nadebryk, E.; Berthomieu, C.; Verméglio, A.; Breton, J. *FEBS Lett.* **1991**, *293*, 53–58.
- (27) Vos, M. H.; Jones, M. R.; Breton, J.; Lambry, J.-C.; Martin, J.-L. *Biochemistry* **1996**, *35*, 2687–2692.
- (28) Joffe, M.; Hulin, D.; Migus, A.; Antonetti, A.; Benoit à la Guillaume, C.; Peyghambarian, N.; Lindberg, M.; Koch, S. W. *Opt. Lett.* **1988**, *13*, 276–278.
- (29) Brito Cruz, C. H.; Gordon, J. P.; Becker, P. C.; Fork, R. L.; Shank, C. V. *IEEE J. Quantum Electron.* **1988**, *24*, 261–266.
- (30) Hamm, P. *Chem. Phys.* **1995**, *200*, 415–429.
- (31) For the exponential fits to the kinetics in this paper, perturbed free induction decay was taken into account by using a function as in eq 1.
- (32) Arnett, D. C.; Moser, C. C.; Dutton, L.; Scherer, N. F. In *Ultrafast Phenomena*; Barbara, P. F., Fujimoto, J. G., Knox, W. H., Zinth, W., Eds.; Springer: Berlin, 1996; Vol. X, pp 334–335.
- (33) Liebl, U.; Lambry, J.-C.; Leibl, W.; Breton, J.; Martin, J.-L.; Vos, M. H. *Biochemistry* **1996**, *35*, 9925–9934.
- (34) Vos, M. H.; Jones, M. R.; Breton, J.; Lambry, J.-C.; Martin, J.-L. In *Ultrafast Phenomena*; Barbara, P. F., Fujimoto, J. G., Knox, W. H., Zinth, W., Eds.; Springer: Berlin, 1996; Vol. X, pp 332–333.
- (35) Vos, M. H.; Jones, M. R.; Hunter, C. N.; Breton, J.; Martin, J.-L. *Proc. Natl. Acad. Sci. U.S.A.* **1994**, *91*, 12701–12705.
- (36) Breton, J. In *The Photosynthetic Bacterial Reaction Center, Structure and Dynamics*; Breton, J., Verméglio, A., Eds.; Plenum: New York, 1988; pp 59–69.
- (37) Although upon direct excitation of P_- the oscillatory features are small at this wavelength, it should be kept in mind that the onset of the SE

occurs with a delay of ~ 70 fs (Figure 4B), reflecting coherent nuclear motion out of the Franck–Condon region. This effect complicates the analysis of rise phases occurring on a similar time scale, as discussed in section 3.2.4. The fact that the observed apparent rise kinetics of ~ 180 fs upon excitation at 770 nm is significantly slower a posteriori justifies the simpler approach of fitting with an exponential function in this case.

(38) Parson, W. W.; Warshel, A. *J. Am. Chem. Soc.* **1987**, *109*, 6152–6163.

(39) Scherer, P. O. J.; Fischer, S. F. In *The Chlorophylls*; Scheer, H., Ed.; CRC: Boca Raton, FL, 1991; pp 1079–1093.

(40) If H and B are coupled, (part of) the bleaching of the B band may reflect H^* . If this were the case, inversely it would be expected that excitation of the B band would lead to intensity changes of the H band (absorption increase if B borrows excitation from $H^{38,39}$ and absorption decrease if H borrows absorption from B). With our 820 nm pulses, which excite P_+ and B (Figure 3), and also in the experiments of Lin et al.²² under more selective excitation of B, absorption changes of the H band are not observed to a significant extent. Therefore, it is reasonable to assume that the bleaching in the B-band region predominantly reflects B^* . We note that whereas theoretical calculations of excitonic interactions in RCs of *Rps. viridis*^{38,39} and *R. sphaeroides*³⁹ indicate considerable mixing of the B and H bands, they were calculated to be weaker than those of the P and B bands discussed in section 4.2.1.

(41) The unknown contributions of SE to the transient spectra associated with the different excited states prevent a precise quantitative analysis of the transient spectra in terms of populations of H^* , B^* , and P_+^* .

(42) Peloquin, J. M.; Lin, S.; Taguchi, A. K. W.; Woodbury, N. W. *J. Phys. Chem.* **1996**, *100*, 14228–14235.

(43) Shreve, A. P.; Cherepy, N. J.; Franzen, S.; Boxer, S. G.; Mathies, R. A. *Proc. Natl. Acad. Sci. U.S.A.* **1991**, *88*, 11207–11211.

(44) Cherepy, N. J.; Shreve, A. P.; Moore, L. J.; Franzen, S.; Boxer, S. G.; Mathies, R. A.; Cherepy, N. J. *J. Phys. Chem.* **1994**, *98*, 6023–6029.

(45) Palaniappan, V.; Schenck, C. C.; Bocian, D. F. *J. Phys. Chem.* **1995**, *99*, 17049–17058.

(46) Upon excitation at 880 nm, the spectral evolution in the 900 nm region is very similar to that described previously for antenna-deficient membranes containing wild-type *R. sphaeroides* RCs upon excitation at 870 nm¹⁹. In the 800 nm region a characteristic double-banded structure appears instantaneously. Using 45 fs pulses centered at 870 nm, we have previously characterized this early-time spectrum and its evolution.²¹ The position and relative amplitude of the two bands are somewhat different in the present work, presumably owing to (a) the different excitation conditions that can modify the transient spectra in the B-band region⁴² and (b) an improved spectral resolution. The spectral resolution in the present work is ~ 1 nm. In ref 21 it was also ~ 1 nm (as mentioned) for the kinetics at single wavelengths, but (as remarked only after the appearance of the paper) somewhat more elevated for the spectra, which were recorded using a different detection setup. The difference in spectral resolution is clearly apparent when comparing the ground-state spectra in the 800 nm region.

(47) Vos, M. H.; Lambry, J.-C.; Robles, S. J.; Youvan, D. G.; Breton, J.; Martin, J.-L. *Proc. Natl. Acad. Sci. U.S.A.* **1991**, *88*, 8888–8889.

(48) Streltsov, A. M.; Aartsma, T. J.; Hoff, A. J.; Shuvalov, V. A. *Chem. Phys. Lett.* **1997**, *266*, 347–352.

(49) The 820 nm pulse excites not only the B and P_+ bands but probably also the P_- band in its extreme high-energy tail. Owing to the substantial inhomogeneous broadening of the P band,³⁰ the absorption of this directly excited P_- population is expected to be blue-shifted with respect to the population excited by a 880 nm pulse.⁴² Indeed, in the 4 ps spectra upon excitation at 880 nm, no bleaching is observed in the 850 nm region (high-energy tail of the P_- band), whereas a bleached area ($\sim 20\%$ of the total P_- bleaching) is observed in this region upon excitation at 820 nm (and at 770 nm). This effect may bias the normalization at 890 nm of Figure 9B and may explain differences in amplitudes of $\sim 20\%$.

(50) Lyle, P. A.; Kolaczowski, S. V.; Small, G. R. *J. Phys. Chem.* **1993**, *97*, 6924–6933.

(51) Feher, G.; Allen, J. P.; Okamura, M. Y.; Rees, D. C. *Nature* **1989**, *339*, 111–116.

(52) Chang, C.-H.; El-Kabbani, O.; Tiede, D.; Norris, J.; Schiffer, M. *Biochemistry* **1991**, *30*, 5353–5369.

(53) Lancaster, C. R. D.; Ermler, U.; Michel, H. In *Anoxygenic Photosynthetic Bacteria*; Blankenship, R. E., Madigan, M. T., Bauer, C. E., Eds.; Kluwer: Dordrecht, 1995; pp 503–526.

(54) In *Rps. viridis* the B, P_+ , and H Q_Y bands are strongly congested at RT as well as at cryogenic temperature, where separate maxima/shoulders, ascribed to P_+ (850 nm), B (834 nm), H_L (805 nm), and H_M (790 nm) can nevertheless be distinguished.²⁵ The $P_- Q_Y$ transition is located at 960 nm (RT) and 990 nm (15 K).

(55) Struve, W. In *Anoxygenic Photosynthetic Bacteria*; Blankenship, R. E., Madigan, M. T., Bauer, C. E., Eds.; Kluwer: Dordrecht, 1995; pp 297–313.

(56) Connolly, J. S.; Samuel, E. B.; Janzen, A. F. *Photochem. Photobiol.* **1982**, *36*, 565–574.

(57) H^* and B^* SE undoubtedly contribute to the early-time transient absorption spectra reported in this paper, but these are too congested for a safe assignment.

(58) In a very recent report⁵⁹ it was described that the bleaching of the P_- ground-state band was, by contrast, not instantaneous upon excitation with 38 fs pulses centered at 799 nm. This indicates that under these conditions P_+ is excited to a much lesser extent than with our 820 nm pulses (in agreement with the idea that it absorbs mainly at the red side of the B band) and, in particular, in the framework of the discussion of section 4.2.1 that B and P_+ are not excited coherently.

(59) Vulto, S. I. E.; Streltsov, A. M.; Shkuropatov, Shuvalov, V. A.; Aartsma, T. J. *J. Phys. Chem.*, in press.

(60) Scherer, P. O. J.; Fischer, S. F. *Chem. Phys. Lett.* **1986**, *131*, 153–159.

(61) Steffen, M. A.; Lao, K.; Boxer, S. G. *Science* **1994**, *264*, 810–816.

(62) Beekman, L. M. P. Ph.D. Thesis, Free University, Amsterdam, 1997.

(63) Leo, K.; Shah, J.; Göbel, E. O.; Damen, T. C.; Schmitt-Rink, S.; Schäfer, W.; Köhler, K. *Phys. Rev. Lett.* **1991**, *66*, 201–204.

(64) The Bchl dimer P is considered a macromolecule in this context, thus “localized in P_+^* ” still implies delocalization over the two Bchls constituting P.

(65) Mar, T.; Picorel, R.; Gingras, G. *Biochemistry* **1993**, *32*, 1466–1470.

(66) Dexter, D. L. *J. Chem. Phys.* **1952**, *21*, 836–850.

(67) Oevering, H.; Verhoeven, J. W.; Paddon-Row, M. N.; Cotsaris, E.; Hush, N. S. *Chem. Phys. Lett.* **1988**, *143*, 488–495.

(68) Johnson, S. G.; Tang, D.; Jankowiak, R.; Hayes, J. M.; Small, G. J.; Tiede, D. *J. Phys. Chem.* **1990**, *94*, 5849–5855.

(69) Since the in vivo redox potential for the reduction of Bphea *a* is higher than that of Bchl *a*,⁷⁰ the formation of $B^+H_L^-$ is more likely than $H_L^+B^-$.

(70) Fajer, J.; Brune, D. C.; Davis, M. S.; Forman, A.; Spaulding, L. D. *Proc. Natl. Acad. Sci. U.S.A.* **1975**, *72*, 4956–4960.

(71) Jackson, J. A.; Lin, S.; Taguchi, A. K. W.; Williams, J. C.; Allen, J. P.; Woodbury, N. W. *J. Phys. Chem. B* **1997**, *101*, 5747–5754.

(72) Holzwarth, A. R.; Müller, M. G. *Biochemistry* **1996**, *35*, 11820–11831.

(73) To our knowledge, for the $P^+H_L^-$ state formed by excitation of the P_- band, no determination of the ratio of the $H_L Q_X$ bleaching and P Q_Y bleaching at low temperature has been published. At RT, where the $H_L Q_Y$ bleaching is also very weak, an approximately stoichiometric ratio for this bleaching can be inferred from the reconstructed 20 ps spectrum of Holzwarth and Muller.⁷²

(74) Warshel, A.; Creighton, S.; Parson, W. W. *J. Phys. Chem.* **1988**, *92*, 2696–2701.

(75) Fischer, S. F.; Scherer, P. O. J. *Chem. Phys.* **1987**, *115*, 151–158.

(76) Alden, R. G.; Hayashi, M.; Allen, J. P.; Woodbury, N. W.; Murchison, H.; Lin, S. H. *Chem. Phys. Lett.* **1993**, *208*, 350–358.

(77) van Grondelle, R.; Dekker, J. P.; Gillbro, T.; Sundström, V. *Biochim. Biophys. Acta* **1994**, *1187*, 1–65.